The Nuclear Magnetic Shielding of the ^{19}F-Nuclei in $KZnF_3$

R. Grosescu * and U. Haeberlen
Max-Planck-Institut für Medizinische Forschung, Abteilung für Molekulare Physik

Z. Naturforsch. **40 a**, 283–293 (1985); received December 20, 1984

Using solid state multiple pulse techniques the magnetic shielding tensors σ of the ^{19}F nuclei in a single crystal of $KZnF_3$ have been measured. The F^--site symmetry in $KZnF_3$, D_{4h}, allows axial anisotropy of σ and determines fully the principal shielding directions. Using CaF_2 as the reference compound, the average shielding is + 85 ppm and the shielding anisotropy is + 18.4 ppm. These results are discussed in terms of shielding contributions from (a) the closed shell electrons of the F^--ion whose shielding is considered, (b) the closed shell electrons of the neighbouring metal and fluorine ions and (c) weak admixture of covalency to the predominantly ionic $Zn^{++}-F^-$ bonding.

1. Introduction

The development of multiple pulse techniques [1, 2] has made possible the measurement of nuclear magnetic shielding tensors of ^{19}F nuclei in the solid state. The ^{19}F shielding has been studied in the past in a variety of compounds with either dominant ionic or covalent bonding, and the results have been discussed in terms of the bonding [3].

In this communication we report on measurements of the shielding tensors of the fluorines in $KZnF_3$. Crystals of this compound are thought to be strongly ionic. We expected and indeed found that the ^{19}F-σ tensors reflect the dominant ionic character of the bonding, but at the same time it is interesting to investigate to what extent the admixture of weak covalency affects the ^{19}F magnetic shielding. A major part of the discussion of our results is concerned with this question.

In most of the *fluorides* studied so far the shielding is isotropic as a result of cubic fluorine site symmetry [3]. In $KZnF_3$ the F^--site symmetry permits an axially symmetric shielding *anisotropy*. Other cases where symmetry permits shielding anisotropy are MgF_2, ZnF_2 and SnF_2. The ^{19}F shielding tensors reported for these compounds [4, 5] are, therefore, best suited for comparison purposes with our results from $KZnF_3$.

By using the radioactive ^{20}F nucleus ($I = 2$) Ackermann et al. [6] have recently measured the electric field gradient (EFG) tensor at the fluorine site in $KZnF_3$. We discuss the question whether and how the nuclear magnetic shielding tensor σ, which can be measured by comparatively simple RF-techniques, can be related to the EFG tensor whose measurement requires techniques and equipment from the arsenal of the nuclear physicist.

2. Symmetry Considerations

$KZnF_3$ has a perowskite-like structure [7]. Figure 1 shows the arrangement of the ions in the unit cell. Each fluorine sits on a fourfold axis which is colinear to the Zn–F–Zn bonds. The local symmetry at the F^--site is D_{4h}. This symmetry imposes *axial* symmetry on the ^{19}F-σ-tensor. Its unique direction must be along the Zn–F–Zn direction, i.e., along one of the primitive crystal axes. There are three symmetry related fluorine ions in the unit

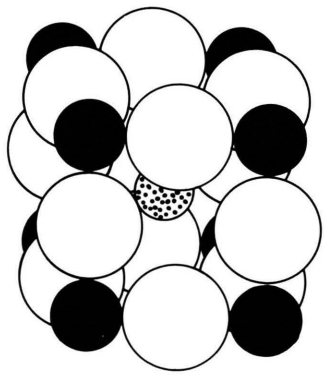

Fig. 1. Packing of the ions in the unit cell of $KZnF_3$. Open spheres: F^-; full spheres: Zn^{++}, speckled sphere: K^+.

* Present address: Central Institute for Physics, Bucharest, Romania.

Reprint requests to Prof. U. Haeberlen, Max-Planck-Institut für Medizinische Forschung, Abteilung für Molekulare Physik, Jahnstraße 29, D-6900 Heidelberg.

0340-4811 / 85 / 0300-0283 $ 01.30/0. – Please order a reprint rather than making your own copy.

cell. As a consequence of this crystal symmetry complete information about the ^{19}F-shielding tensor $\boldsymbol{\sigma}$ can be obtained from a single spectrum taken with B_0 parallel to one of the crystal axes, e.g., $B_0 \parallel 100$. For such a crystal orientation B_0 is *parallel* to the Zn−F−Zn direction of one, and *perpendicular* to the Zn−F−Zn directions of the other two of the three F^--ions in the unit cell, see Figure 1. For this orientation we expect, hence, *two* NMR lines with an intensity ratio of 1 : 2. The smaller of the lines reflects $\sigma_\parallel$, the larger $\sigma_\perp$, their separation gives directly the shielding anisotropy $\Delta\sigma = \sigma_\parallel - \sigma_\perp$.

According to these considerations we prepared a sample crystal such that its c-axis was parallel to the NMR goniometer axis which itself is perpendicular to $\boldsymbol{B}_0$. This allows to align the a- as well as the b-axis of the crystal parallel to $\boldsymbol{B}_0$.

For a general orientation of the crystal relative to $\boldsymbol{B}_0$ we expect three NMR lines. All these lines must coincide for $B_0 \parallel (111)$.

3. Experimental and Results

The ^{19}F high resolution NMR measurements were performed on a 90 MHz Bruker pulse spectrometer modified for multiple pulse experiments. The spectra were obtained with a phase error and flip-angle error self correcting version of the MREV cycle [2]. The width of the $\pi/2$ pulses was 0.8 μsec, their separation 3 μsec and 6 μsec, respectively. This method averages out the ^{19}F-^{19}F homonuclear part of the dipole-dipole Hamiltonian. The heteronuclear dipole interactions, ^{19}F-^{67}Zn and ^{19}F-$^{39,41}K$, are only scaled down by a factor of $\sqrt{2}/3$. The shortest internuclear distances, and hence potentially the strongest DD interactions, are between the ^{19}F and Zn nuclei. Fortunately, the natural abundance of the magnetic Zn isotope ^{67}Zn is only 4.12% so that most of the ^{19}F nuclei have non-magnetic Zn isotopes as their nearest neighbours. The other non-averaged dipolar interaction, between K and F nuclei, is weak since the shortest K−F distance in $KZnF_3$ is rather large ($a/\sqrt{2}$ with $a = 4.055$ Å) and the gyromagnetic ratios of both the ^{39}K and ^{41}K isotopes are small. These interactions, nevertheless, limit the resolution in our spectra. A second moment calculation of the K−F interactions accounts well for the observed linewidths.

A spectrum for $\boldsymbol{B}_0 \parallel (100)$ is shown in Figure 2. It shows indeed two lines with the expected intensity ratio of 2 : 1. The separation of the lines is 18.4 ppm and corresponds, as mentioned above, directly to $\Delta\sigma$. Further spectra were recorded for different orientations of $\boldsymbol{B}_0$ in the $a-b$ plane. The analysis of the rotation pattern of the line shifts helped to minimize errors in our final numbers which resulted from a small misorientation of the sample crystal. A sphere of a single crystal of CaF_2 was used as the reference compound.

The chemical shift tensor of the ^{19}F nuclei in $KZnF_3$ derived from our data is given in Table 1. In order to compare our results with theoretical calculations the principal values of $\boldsymbol{\sigma}$ must be given on an absolute scale. For ^{19}F such a scale was established by Hindermann et al. [8]. The second line of Table 1 gives $\boldsymbol{\sigma}$ in $KZnF_3$ on this scale.

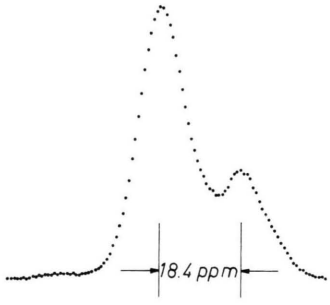

Fig. 2. Multiple pulse spectrum of a single crystal of $KZnF_3$; $\boldsymbol{B}_0$ parallel (100).

Table 1. ^{19}F shielding tensor in $KZnF_3$ (all units in ppm).

	$\sigma_\parallel$	$\sigma_\perp$	$\Delta\sigma$	$\bar{\sigma}$
Experimental reference: CaF_2	97.4	78.8	18.6	85
Experimental absolute scale [a]	390	371.4	18.6	377.6
Contributions				
1. closed shell F^--ion	480.2	480.2	0	480.2
2. geometrical [b]	7.3	−3.1	10.4	~0.3
3. departure from pure ionic model [c]	−97.5	−105.7	8.2	−102.97
4. diamag. (overlap and covalency)	~2.1	~1.6	~0.5	~1.6
5. paramagnetic (overlap and covalency)	−99.6	−107.3	7.7	−104.57

[a] Absolute scale according to [8].
[b] Calculated using Pascal's constants.
[c] Obtained by subtracting contributions 1 and 2 from the experimental values on the absolute scale.

4. Discussion

The main features of our experimental results may be summarized as follows:

- the unique axis of the axially symmetric ^{19}F-$\boldsymbol{\sigma}$-tensor corresponds to the *most shielded* direction and is along the "bonding" direction Zn−F−Zn.
- the *anisotropy* of $\boldsymbol{\sigma}$ is *small* compared with the size of the individual components of $\boldsymbol{\sigma}$ taken on the *absolute scale.*

The feature of the ^{19}F-$\boldsymbol{\sigma}$-tensor which reflects most directly the *ionic* nature of the bonding in $KZnF_3$ is the small size of $\Delta\sigma$. This can be seen by analysing the different contributions to $\boldsymbol{\sigma}$, see further below, but also on a simple comparative basis. Other fluorides whose ^{19}F shielding has been investigated by high resolution solid state NMR and where crystal symmetry does not prohibit shielding *anisotropy* are MgF_2, ZnF_2 and SnF_2. In neither of these compounds crystal symmetry forces $\boldsymbol{\sigma}$ to be axially symmetric. MgF_2 and ZnF_2 are typical ionic compounds, the differences between the largest and the smallest ^{19}F principal shielding components are 30 ppm (MgF_2) and 44 ppm (ZnF_2), see [4]. SnF_2, on the other hand, forms rings of tetramers, Sn_4F_8, with four different fluorine sites. The shielding anisotropies, $\Delta\sigma = 210$, 165, 106 and 97 ppm (sites 1−4) are comparable in size to the shielding anisotropies of typically covalently bound fluorides, see Table 5.4 of [1]. Along with other evidence the "large" shielding anisotropies measured in SnF_2 have, consequently, been interpreted as signalizing predominantly covalent bonding of the Sn_4F_8 tetramers. The shielding anisotropy, and, of course, plenty other chemical and physical evidence as well, puts $KZnF_3$ in one class with MgF_2 and ZnF_2, i.e., in the class of predominantly ionic fluorides.

We proceed by analysing the origin of different contributions to $\boldsymbol{\sigma}$ in $KZnF_3$.

According to the general theory of the chemical shift [9], $\boldsymbol{\sigma}$ can be split into a dia- and into a paramagnetic term:

$$\boldsymbol{\sigma} = \boldsymbol{\sigma}^{\mathrm{d}} + \boldsymbol{\sigma}^{\mathrm{p}}\,, \tag{1}$$

where

$$\sigma_{ij}^{\mathrm{d}} = \frac{e^2}{2mc^2}\left\langle \psi_0 \middle| \sum_k \frac{r_k^2\,\delta_{ij} - r_{ki}\cdot r_{kj}}{r_k^3} \middle| \psi_0 \right\rangle \tag{2}$$

and

$$\sigma_{ij}^{\mathrm{p}} = \frac{e^2}{2m^2c^2}\sum_m (E_0 - E_m)^{-1} \cdot \left\{ \left\langle \psi_0 \middle| \sum_k l_{ki} \middle| \psi_m \right\rangle \left\langle \psi_m \middle| \sum_k l_{kj}/r_k^3 \middle| \psi_0 \right\rangle + \left\langle \psi_0 \middle| \sum_k l_{ki}/r_k^3 \middle| \psi_m \right\rangle \left\langle \psi_m \middle| \sum_k l_{kj} \middle| \psi_0 \right\rangle \right\}. \tag{3}$$

ψ_0 and ψ_m are the ground- and excited wave functions of the system in the absence of the external field $\boldsymbol{B}_0$; $\boldsymbol{r}_k$ is the vector from the nucleus under consideration to the k-th electron; l_{ki} is the i-component of the angular momentum operator of the electron k about the nucleus of interest.

$\boldsymbol{\sigma}^{\mathrm{d}}$ involves an average over the ground state ψ_0, whereas the calculation of $\boldsymbol{\sigma}^{\mathrm{p}}$ requires knowledge of the excited states. In order to avoid the use of excited states which in general are not known, one often takes recourse to the so-called closure approximation. The paramagnetic term then becomes

$$\sigma_{ij}^{\mathrm{p}} = -\frac{e^2}{\Delta m^2 c^2}\sum_{k,k'}\left\langle \psi_0 \middle| l_{ki}\, l_{k'j}/r_k^3 \middle| \psi_0 \right\rangle, \tag{4}$$

where the average is taken again over only the ground state ψ_0. The "average" energy splitting Δ must be interpreted as a parameter. ψ_0 is written as a single determinant of molecular orbitals (MO) ψ_j:

$$\psi_0 = (2n!)^{-1/2} \cdot \left| \psi_1(1)\,\alpha(1)\,\psi_1(2)\,\beta(2)\ldots\psi_n(2n)\,\beta(2n) \right|, \tag{5}$$

where α and β correspond to the two orientations of the electron spin.

The doubly filled molecular orbitals ψ_j will be approximated by linear combinations of atomic orbitals (MO-LCAO):

$$\psi_j = \sum_{l\alpha} A_l^{\alpha}(j)\,\varphi_l^{\alpha}\,, \tag{6}$$

where φ_l^{α} is an atomic (ionic) wave function of α-type centered on nucleus l.

Using (2) − (6) we get

$$\sigma_{ij}^{\mathrm{d}} = \frac{e^2}{2mc^2}\sum_{l\alpha}\sum_{k\beta} P_{lk}^{\alpha\beta}\left\langle \varphi_k^{\beta} \middle| \frac{r^2\,\delta_{ij} - r_i\,r_j}{r^3} \middle| \varphi_l^{\alpha} \right\rangle, \tag{7}$$

$$\sigma_{ij}^{\mathrm{p}} = -\frac{e^2}{\Delta m^2 c^2}\left[\sum_{l\alpha}\sum_{k\beta} P_{lk}^{\alpha\beta}\left\langle \varphi_k^{\beta} \middle| l_i\, l_j/r^3 \middle| \varphi_l^{\alpha} \right\rangle - \tfrac{1}{2}\sum_{\substack{l\alpha\\ l'\alpha'}}\sum_{\substack{k\beta\\ k'\beta'}} P_{lk}^{\alpha\beta}\, P_{l'k'}^{\alpha'\beta'} \cdot \left\langle \varphi_k^{\beta} \middle| l_i/r^3 \middle| \varphi_{l'}^{\alpha'} \right\rangle \left\langle \varphi_{k'}^{\beta'} \middle| l_j \middle| \varphi_l^{\alpha} \right\rangle \right], \tag{8}$$

where the $P_{lk}^{\alpha\beta} = \sum_j 2A_l^\alpha(j)\,A_k^{*\beta}(j)$ are the matrix elements of the charge density matrix $\boldsymbol{P}$ [10].

If the $A_l^\alpha(j)$ are real then $P_{lk}^{\alpha\beta} = P_{kl}^{\beta\alpha}$. Before discussing different possibilities of constructing MOs for $KZnF_3$ we consider the order of magnitude of different terms in (7)–(8), disregarding the size of $P_{lk}^{\alpha\beta}$.

Label the nucleus of interest as $l = 0$, then:

- $\langle\varphi_0^\beta \mid l_j \mid \varphi_0^\alpha\rangle$ either zero or of the order of $\langle\varphi_0^\alpha \mid \varphi_0^\alpha\rangle = 1$.
- $\langle\varphi_0^\alpha \mid \frac{r^2\delta_{ij} - r_i r_j}{r^3} \mid \varphi_0^\beta\rangle$ and $\langle\varphi_0^\alpha \mid \frac{l_i}{r^3} \mid \varphi_0^\alpha\rangle$ are either zero or are of the order of $\langle 1/r\rangle_0$ and $\langle 1/r^3\rangle_0$, respectively.
- $\langle\varphi_l^\alpha \mid l_j \mid \varphi_0^\beta\rangle$ either zero or of the order of $\langle\varphi_l^\alpha \mid \varphi_0^\beta\rangle = S_{l0}^{\alpha\beta}$ (overlap integral). The $S_{l0}^{\alpha\beta}$ are two center integrals.
- $\langle\varphi_l^\alpha \mid l_i/r^3 \mid \varphi_l^\beta\rangle$ is of the order of $\langle\varphi_l^\alpha \mid 1/r^3 \mid \varphi_l^\alpha\rangle$.

This again is a two-center integral but much smaller than $\langle 1/r^3\rangle_0$.

All other terms are either three-center integrals or products of two-center integrals.

Therefore the main contributions in (7) and (8) are expected to come from terms proportional to $\langle 1/r\rangle_0$, $\langle 1/r^3\rangle_0$ or $\langle\varphi_l^\alpha \mid 1/r \mid \varphi_l^\beta\rangle$ and from those which contain products of the form $\langle 1/r^3\rangle_0 \cdot S_{l0}^{\alpha\beta}$. Since the local symmetry of the F^{19}-nucleus in $KZnF_3$ is D_{4h}, we are interested only in σ_{xx} and σ_{zz}. As the nucleus of interest ($l = 0$) is F^{19} we shall take as basis for φ_0^α the set $|2s\rangle$, $|2p_x\rangle$, $|2p_y\rangle$, $|2p_z\rangle$. Retaining only the contributions linear in $\langle 1/r\rangle_0$, $\langle 1/r^3\rangle_0$ and $\langle\varphi_l^\alpha \mid 1/r \mid \varphi_l^\beta\rangle$, (7) and (8) can be brought into the following form:

$$\sigma_{xx}^{\mathrm{d}} = \frac{e^2}{2mc^2}\sum_{l\alpha} P_{ll}^{\alpha\alpha}\left\langle\varphi_l^\alpha \mid \frac{r^2 - x^2}{r^3} \mid \varphi_l^\alpha\right\rangle, \tag{10}$$

$$\sigma_{zz}^{\mathrm{d}} = \frac{e^2}{2mc^2}\sum_{l\alpha} P_{ll}^{\alpha\alpha}\left\langle\varphi_l^\alpha \mid \frac{r^2 - z^2}{r^3} \mid \varphi_l^\alpha\right\rangle \tag{11}$$

and

$$\begin{aligned}\sigma_{xx}^{\mathrm{p}} = &-\frac{e^2\hbar^2}{\Delta m^2 c^2}\langle 1/r^3\rangle_0 \\ &\cdot\Big\{[P_{00}^{yy} + P_{00}^{zz} - (P_{00}^{yy}P_{00}^{zz} - P_{00}^{yz}P_{00}^{zy})] \\ &\quad - \Big[\sum_{l\alpha}(P_{00}^{zz}P_{l0}^{\alpha y} - P_{00}^{yz}P_{l0}^{\alpha z})\,S_{l0}^{\alpha y} \\ &\qquad + (P_{00}^{yy}P_{l0}^{\alpha z} - P_{00}^{zy}P_{l0}^{\alpha y})\,S_{l0}^{\alpha z}\Big] \\ &\quad + \Big[\sum_l\sum_{\alpha,\beta} P_{l0}^{\alpha z}P_{l0}^{\beta y}\,\langle\varphi_l^\beta \mid l_x \mid \varphi_l^\alpha\rangle \mid m/\hbar\Big]\Big\},\end{aligned} \tag{12}$$

$$\begin{aligned}\sigma_{zz}^{\mathrm{p}} = &-\frac{e^2\hbar^2}{\Delta m^2 c^2}\langle 1/r^3\rangle_0 \\ &\cdot\Big\{[P_{00}^{xx} + P_{00}^{yy} - (P_{00}^{xx}P_{00}^{yy} - P_{00}^{xy}P_{00}^{yx})] \\ &\quad - \Big[\sum_{l\alpha}(P_{00}^{xx}P_{l0}^{\alpha y} - P_{00}^{yx}P_{l0}^{\alpha x})\,S_{l0}^{\alpha y} \\ &\qquad + (P_{00}^{yy}P_{l0}^{\alpha x} - P_{00}^{xy}P_{l0}^{\alpha y})\,S_{l0}^{\alpha x}\Big] \\ &\quad + \Big[\sum_l\sum_{\alpha\beta} P_{l0}^{\alpha y}P_{l0}^{\beta x}\,\langle\varphi_l^\beta \mid l_z \mid \varphi_l^\alpha\rangle \mid m/\hbar\Big]\Big\}.\end{aligned} \tag{13}$$

The calculation of $P_{lk}^{\alpha\beta}$ requires the knowledge of ψ_j. The MOs ψ_j may be constructed by different methods. Since $KZnF_3$ is mainly ionic we shall consider the following approximations:

A) The wavefunctions ψ_j are *purely* ionic. In this approximation the non-orthogonality of MOs on different nuclei is disregarded.

B) The MOs are obtained by Löwdin's orthogonalization method [11]. The ψ_j are still mainly ionic but orthogonal.

C) Covalent bonding between F^- and Zn^{++} electrons is taken into account. We shall discuss approximations A to C in turn.

A) If ψ_j is purely ionic $\psi_j = \varphi_l^\alpha$ and $P_{ll}^{\alpha\alpha} = 2$, $P_{lk}^{\alpha\beta} = 0$.

Equations (10)–(13) become

$$\sigma_{xx}^{\mathrm{d}} = \frac{2e^2}{mc^2}\left[\sum_\alpha\left\langle\varphi_0^\alpha \mid \frac{r^2 - x^2}{r^3} \mid \varphi_0^\alpha\right\rangle + \sum_{l\alpha}^{l\neq 0}\left\langle\varphi_l^\alpha \mid \frac{r^2 - x^2}{r^3} \mid \varphi_l^\alpha\right\rangle\right], \tag{14}$$

$$\sigma_{zz}^{\mathrm{d}} = \frac{2e^2}{mc^2}\left[\sum_\alpha\left\langle\varphi_0^\alpha \mid \frac{r^2 - z^2}{r^3} \mid \varphi_0^\alpha\right\rangle + \sum_{l\alpha}^{l\neq 0}\left\langle\varphi_l^\alpha \mid \frac{r^2 - z^2}{r^3} \mid \varphi_l^\alpha\right\rangle\right], \tag{15}$$

$$\sigma_{xx}^{\mathrm{p}} = \sigma_{zz}^{\mathrm{p}} = 0.$$

The first terms in (14) and (15) are the ionic contributions due to the closed shells of electrons on the F^--ion under investigation. For these terms we rely on work of Sidwell and Hurst [12] who obtained σ_{xx}^{d} (free ion) = σ_{zz}^{d} (free ion) = 480 ppm.

The second terms in (14) and (15) are the contributions from the closed shells of neighbouring ions. These contributions, sometimes called „geometrical" can be calculated by inserting appropriate wave functions in (14)−(15) and integration. This procedure was used in [4] for MgF_2. To take account of these contributions, we shall use the phenomenological magnetic dipole model [13]. In this model induced magnetic dipoles are assigned to individual ions. The fields associated with these dipoles give the following contribution to the shielding of the nucleus of interest:

$$\boldsymbol{\sigma}(\mathrm{g}) = \boldsymbol{\sigma}^{\mathrm{d}}(\mathrm{g}) = 1/L \sum_k (\boldsymbol{\chi}^k/R_k^3 - 3\,(\boldsymbol{\chi}^k\,\boldsymbol{R}_k)\,\boldsymbol{R}/R^5)\,. \tag{16}$$

g means "geometrical", L is Loschmidt's number, $\boldsymbol{\chi}^k$ the molar susceptibility of the k-th ion. For the evaluation of $\boldsymbol{\sigma}$(g) we used for the susceptibilities Pascal's constants [14]. The summation was extended over 50 neighbours. The results are given in line 4 of Table 1.

Note that the values of $\sigma_{\parallel}^{\mathrm{d}}$ (g) and $\sigma_{\perp}^{\mathrm{d}}$ (g) are *small* compared with the experimental ones on the absolute scale and as well small compared with σ (free ion). Note also that the anisotropy $\Delta\sigma^{\mathrm{d}}$ (g) is comparable in size with $\Delta\sigma$ (exptl.).

In order to check the reliability of the dipole model we calculated $\boldsymbol{\sigma}^{\mathrm{d}}$ (g) for MgF_2 using (16) and compared the results with those of [4] obtained by integration. The two methods give results which differ by no more than 1−2 ppm. We do not consider differences of this size as essential.

$\boldsymbol{\sigma}^{\mathrm{d}}$ (free ion) and $\boldsymbol{\sigma}^{\mathrm{d}}$ (g) appear unchanged in the approximation of MOs to be discussed now and therefore will not be considered anymore.

The values reported in the fifth line of Table 1 are obtained by substracting $\boldsymbol{\sigma}^{\mathrm{d}}$ (free ion) and $\boldsymbol{\sigma}^{\mathrm{d}}$ (g) from the experimental values. They reflect the contributions brought in by the departure of the wave functions from their purely ionic form and will be referred to henceforth as "non-ionic contributions".

B) Löwdin's orthogonalization method [11] provides the following set of wave functions

$$\psi_j = \psi_l^{\alpha} = \varphi_l^{\alpha} - \tfrac{1}{2}\sum_{k\beta} S_{kl}^{\beta\alpha}\,\varphi_k^{\beta} + \tfrac{3}{8}\sum_{k\beta}\sum_{n\gamma} S_{kn}^{\beta\gamma}\,S_{nl}^{\gamma\alpha}\,\varphi_k^{\beta} + \ldots \tag{17}$$

which leads to

$$P_{00}^{\alpha\alpha} = 2\left[1 + \sum_{l'\alpha'} (S_{l'0}^{\alpha'\alpha})^2\right],$$

$$P_{00}^{\alpha\beta} = 2\sum_{l'\alpha'} S_{l'0}^{\alpha'\alpha}\,S_{l'0}^{\alpha'\beta},$$

$$P_{l0}^{\alpha\beta} = -2\left[S_{l0}^{\alpha\beta} - \sum_{l'\alpha'} S_{ll'}^{\alpha\alpha'}\,S_{l'0}^{\alpha'\beta}\right]. \tag{18}$$

using (18) and (10)−(13) one obtains

$$\sigma_{xx}^{\mathrm{d}} = \frac{4}{5}\frac{e^2}{m\,c^2}\langle 1/r\rangle_{\mathrm{F}_{2\mathrm{p}}} \cdot \sum_{l\alpha}\left[|\,S_{l0}^{\alpha y}\,|^2 + |\,S_{l0}^{\alpha z}\,|^2 + \tfrac{1}{2}\,|\,S_{l0}^{\alpha x}\,|^2\right], \tag{20}$$

$$\sigma_{xx}^{\mathrm{p}} = -\frac{2e^2\hbar^2}{\Delta\,m^2\,c^2}\langle 1/r^3\rangle_{\mathrm{F}_{2\mathrm{p}}}\sum_{l\alpha}\left[|\,S_{l0}^{\alpha y}\,|^2 + |\,S_{l0}^{\alpha z}\,|^2 + \frac{2m}{\hbar}\sum_{\beta} S_{l0}^{\alpha z}\,S_{l0}^{\beta y}\,|\langle\varphi_l^{\beta}|\,l_x\,|\varphi_l^{\alpha}\rangle|\right], \tag{21}$$

and corresponding expressions for σ_{zz}^{d} and σ_{zz}^{p}.

In (17)−(21) all terms containing overlap integrals of power higher than two were neglected. The contributions of different neighbours are additive. It should be noted that the same result is obtained if one uses a simpler set of wave functions which ensures only the orthogonality of wave functions on neighbouring ions with those on the ion of interest ($l = 0$):

$$\psi_0^{\alpha} = \varphi_0^{\alpha},$$

$$\psi_l^{\alpha} = \left[\varphi_l^{\alpha} - \sum_{\beta} S_{l0}^{\alpha\beta}\,\varphi_0^{\beta}\right] \Big/ \left(1 - \sum_{\beta}(S_{l0}^{\alpha\beta})^2\right)^{1/2}. \tag{22}$$

The equivalence appears immediately if one observes that within the same approximations (22) leads to

$$P_{00}^{\beta\beta} = 2\left[1 + \sum_{l\alpha} |\,S_{l0}^{\alpha\beta}\,|^2\right], \quad \text{etc.}$$

The set of wave functions given by (17) and their consequence, (20) and (21) have been widely used in chemical shift calculations in many predominantly ionic crystals [4, 15, 16]. Nevertheless, (17) or its simplified form, (22) excludes any covalent effects which in the case of metal-halogen (Zn-F) bonding may be of the same order of magnitude as the overlap contributions as far as the *anisotropy* $\Delta\sigma$ is concerned. Therefore, detailed evaluations of 20 and 21 will be given once the covalency effect is taken into account. In fact, our calculations (see further below) have shown that (20) leads to negligibly small contributions to $\Delta\sigma^{\mathrm{d}}$ and $\bar{\sigma}^{\mathrm{d}}$ as expected [15, 16]. On the

other hand, (21) leads to a calculated value of the ratio $\Delta\sigma^p/\bar{\sigma}^p$ which is almost one order of magnitude smaller than that obtained with the semi-experimental numbers from line 5 of Table 1, and the sign is opposite. Therefore we looked for possible effects of weak covalent bonding between Zn^{++} and F^-.

C) Covalency may make an important input to the chemical shift tensor since it leads to a strong delocalization of electrons and therefore to a more important departure of the wave functions from their ionic form than that predicted by (17).

In the case of KXF_3 crystals it was shown [17] that covalency arises mainly from the interactions between (2s, 2p)-electrons of the F^- and 3d-electrons of the X^{++}-ions, leading to bonding and antibonding states. We consider only the interactions between F^- (0, 0, 0) and its two Zn-neighbours at $(0, 0, \pm\frac{1}{2})$. The bonding (b) and antibonding (a) MOs which transform according to irreducible representations of D_{4h} (F^--site symmetry) are:

$$\psi_r^b(e_u) = 1/\sqrt{N^b(e_u)}\ [|p_r\rangle + b_r|\chi_r\rangle], \quad (r = x, y) \tag{23}$$

$$\begin{aligned}\psi_r^a(e_u) &= 1/\sqrt{N^a(e_u)}\ [|\chi_r\rangle - a_r|p_r\rangle],\\ \psi_z^b(a_{2u}) &= 1/\sqrt{N^b(a_{2u})}\ [|p_z\rangle + b_z|\chi_z\rangle],\\ \psi_z^a(a_{2u}) &= 1/\sqrt{N^a(a_{2u})}\ [|\chi_z\rangle - a_z|p_z\rangle]\end{aligned} \tag{24}$$

with

$$\begin{aligned}\chi_r(e_u) &= 1/\sqrt{2}\,[d_{rz}(+\tfrac{1}{2}) + d_{rz}(-\tfrac{1}{2})],\\ \chi_z(a_{2u}) &= 1/\sqrt{2}\,[d_{z^2}(+\tfrac{1}{2}) - d_{z^2}(-\tfrac{1}{2})].\end{aligned} \tag{25}$$

The normalization factors are:

$$N_\alpha^b = 1 + b_\alpha^2 + 2b_a S_\alpha, \quad N_\alpha^a = 1 + a_\alpha^2 - 2a_\alpha S_\alpha$$

with $a_\alpha = (b_\alpha + S_a)/(1 + b_\alpha S_\alpha)$ and $S_\alpha = \langle p_\alpha|\chi_\alpha\rangle$. The wave functions of electrons on neighbour ions, K^+ and F^-, which do not participate in the bonding are taken of the form (22) in order to ensure orthogonality. This set of wave functions leads to the following result:

$$\begin{aligned}\sigma_{xx}^p &= \sigma_{xx}^p(N) + \sigma_{xx}^p(Zn),\\ \sigma_{zz}^p &= \sigma_{zz}^p(N) + \sigma_{zz}^p(Zn).\end{aligned} \tag{26}$$

$\sigma_{xx}^p(N)$ and $\sigma_{zz}^p(N)$ are given by (21) and reflect the overlap contributions of K^+ and F^--neighbours. The second terms in (26) are:

$$\begin{aligned}\sigma_{xx}^p(Zn) &= -\frac{4e^2\hbar^2}{\Delta m^2 c^2}\langle 1/r^3\rangle_{F_{2p}}\\ &\quad\cdot[|S_{10}^{z^2,z}|^2 + |S_{10}^{yz,z}|^2 - 2\sqrt{3}\,S_{10}^{z^2,z}S_{10}^{yz,y}],\\ \sigma_{zz}^p(Zn) &= -\frac{4e^2\hbar^2}{\Delta m^2 c^2}\langle 1/r^3\rangle_{F_{2p}}\\ &\quad\cdot[|S_{10}^{xz,x}|^2 + |S_{10}^{yz,y}|^2 - 2S_{10}^{xz,x}S_{10}^{yz,y}].\end{aligned} \tag{27}$$

$S_{10}^{\alpha\beta}$ stands for the overlap integral between the d_α wave function of Zn^{++} at $(0, 0, +\frac{1}{2})$ and the p_β-wave function of F^- at (0, 0, 0).

This result is easily obtained if one observes that the set of wave functions (22) and (23) – (25) gives

$$P_{00}^{\alpha\alpha} = 2\left[1/N_\alpha^b + a_\alpha^2/N_\alpha^a + \sum_{k\beta}|S_{k0}^{\beta\alpha}|^2\right]$$

(k runs over the K^+, F^--neighbours),

$$P_{l0}^{\alpha\alpha} = 2\,[b_\alpha/\sqrt{2N_\alpha^b} - a_\alpha/\sqrt{2N_\alpha^a}] \quad \text{for } l = 1, 2\ (Zn^{++})$$

and

$$P_{l0}^{\alpha\beta} = -2\,S_{l0}^{\alpha\beta} \quad \text{for } l \neq 1, 2\ (Zn^{++})$$

which, when inserted in (8), give (26) and (27).

In fact, the result of (27) is also contained in (20) and (21). The summations in the latter equations include the Zn^{++}-neighbours and it can be easily shown that their contributions are identical to (27). It shows that for weak covalent bonding, as long as one considers fully occupied bonding and antibonding states, the final result depends only on overlaps between neighbours and is entirely equivalent to that obtained with Löwdin's set of wave functions (at least within the present approximations).

It should be noted that the MOs given in (23) to (24) imply a (slight) delocalization of the electrons on the F^--ion which results entirely from mixing of F^--AOs and Zn^{++}-AOs. That this is the dominant delocalization is questionable since many results obtained by N.M.R., E.P.R. and optical methods in KXF_3-crystals (X = Mn, Ni) could be explained by weak covalent bonding between the central ion (X) and its six next fluorine neighbour ions whose electrons were assumed to occupy *ligand* orbitals (17). Ligand orbitals imply a stronger delocalization than that given by (23). In fact, in these works the covalency effects were investigated within the fragment XF_6 (O_h-symmetry). Therefore we considered it interesting to evaluate the chemical shift of F^{19} in

this fragment (X = Zn) using the same type of wave functions as in the above mentioned works and to compare the results with those obtained with the previous sets of wave functions as given by (17) and (23)–(25). The calculations carried out in the Appendix give a result which is equivalent to (26) and (27) as long as the bonding and antibonding states are fully occupied. The main advantage of considering F^--ligand orbitals is that one may easily envisage the effects of non-occupied antibonding states. We shall turn to this point now, discussing it for the XF_6 fragment. An unoccupied antibonding state may arise from the excited state $|4s\rangle$ of Zn^{++}. This state transforms according to the a_{1g}-irreducible representation of O_h and can be coupled to the F^--ligand state $\chi(a_{1g})$ to form a bonding-antibonding pair in which only the bonding state is occupied. It can be shown that in this case (see Appendix) σ^p_{zz} remains unchanged with regard to (26), whereas σ^p_{xx} has an additional contribution given by:

$$\sigma^p_{xx}(\text{cov.}) = -\frac{4e^2\hbar^2}{\Delta m^2 c^2}\langle 1/r^3\rangle_0 \cdot \tfrac{1}{6} \cdot b^2(a_{1g}) \quad (28)$$

where $b(a_{1g})$ is the covalency factor [17] specific to the a_{1g}-states. In the following it will be simply labelled as b. Taking into account this contribution, the expressions used for numerical evaluations are:

$$\sigma^p_{xx} = \sigma^p_{xx}(O) - \frac{2e^2\hbar^2}{\Delta m^2 c^2}\langle 1/r^3\rangle_0 \cdot \tfrac{1}{3} b^2\,, \quad (29)$$

$$\sigma^p_{zz} = \sigma_{zz}(O)\,,$$

where $\sigma^p_{xx}(O)$ and $\sigma^p_{zz}(O)$ are given by (21).

The overlaps in (29) and (21) will be restricted to outer shells, namely: 3d for Zn^{++}, (3s, 3p) for K^+ and (2s, 2p) for F^-.

The summation in (29) was taken over the following groups of neighbours: two Zn^{++} labelled (1, 2) at $(0, 0, \pm\frac{1}{2})$, two F^- (1, 2) at $(0, 0, \pm 1)$, four K^+ (1–4) at $(+\frac{1}{2}, +\frac{1}{2}, 0)$ and symmetry related positions, and eight F^- (1–8) at $(+\frac{1}{2}, 0, -\frac{1}{2}; 0, +\frac{1}{2}, -\frac{1}{2})$ and symmetry related positions). The overlap properties which arise from the symmetry of the problem (e.g., $|S^{xz,x}_{10}|^2 = |S^{xz,x}_{20}|^2$ for Zn^{++}, ect.) allow to bring (29) to a form which reflects the contributions of different groups of neighbours:

$$\sigma^p_{xx} = -\frac{2e^2\hbar^2}{\Delta m^2 c^2}\langle 1/r^3\rangle$$
$$\cdot \{2[|S^{yz,y}_{10}|^2 + |S^{z^2,z}_{10}|^2 - 2\sqrt{3}\,S^{yz,z}_{10}S^{z^2,z}_{10} + b^2/6]_{2\times Zn^{++}}$$
$$+ 4[|S^{sy}_{10}|^2 + |S^{xy}_{10}|^2 + |S^{yy}_{10}|^2 + |S^{zz}_{10}|^2 - 2S^{yy}_{10}S^{zz}_{10}]_{4\times K^+}$$
$$+ 2[|S^{sz}_{10}|^2 + |S^{yy}_{10}|^2 + |S^{zz}_{10}|^2 - 2S^{yy}_{10}S^{zz}_{10}]_{2\times F^-}$$
$$+ 4[|S^{sz}_{10}|^2 + |S^{xz}_{10}|^2 + |S^{yy}_{10}|^2 + |S^{zz}_{10}|^2 - 2S^{yy}_{10}S^{zz}_{10}$$
$$+ |S^{sy}_{20}|^2 + |S^{zy}_{20}|^2 + |S^{yz}_{20}|^2 + |S^{yy}_{20}|^2 + |S^{zz}_{20}|^2$$
$$- 2(S^{zy}_{20}S^{yz}_{20} + S^{yy}_{20}S^{zz}_{20})]_{8\times F^-}\} \quad (30)$$

$$\sigma^p_{zz} = -\frac{2e^2\hbar^2}{\Delta m^2 c^2}\langle 1/r^3\rangle_0$$
$$\cdot \{2[|S^{xz,x}_{10}|^2 + |S^{yz,y}_{10}|^2 - 2S^{xz,x}_{10}S^{yz,y}_{10}]_{2\times Zn^{++}}$$
$$+ 4[|S^{sx}_{10}|^2 + |S^{sy}_{10}|^2 + |S^{xx}_{10}|^2 + |S^{yy}_{10}|^2 - 2S^{xx}_{10}S^{yy}_{10}]_{4\times K^+}$$
$$+ 2[|S^{xx}_{10}|^2 + |S^{yy}_{10}|^2 - 2S^{xx}_{10}S^{yy}_{10}]_{2\times F^-}$$
$$+ 4[|S^{sx}_{10}|^2 + |S^{zx}_{10}|^2 + |S^{xx}_{10}|^2 + |S^{yy}_{10}|^2$$
$$- 2S^{xx}_{10}S^{yy}_{10} + |S^{sy}_{20}|^2 + |S^{zy}_{20}|^2 + |S^{xx}_{20}|^2 + |S^{yy}_{20}|^2$$
$$- 2S^{xx}_{20}S^{yy}_{20}]_{8\times F^-}\}\,. \quad (31)$$

The indices 1 or 2 in each square bracket signify the nucleus at position 1 or 2 in each group according to the previous notation.

Overlap integrals are usually reported in terms of $S^{\pi\pi}$, $S^{\sigma\sigma}$ or $S^{\delta\sigma}$, (17) and (18). Since in general the z-axis of the crystal frame used to write the ionic functions does not coincide with the vector between two nuclei, we made the necessary transformations to express different $S^{\alpha\beta}_{lk}$ in terms of these standard overlaps. We give the result directly for $\Delta\sigma^p$ and $\bar{\sigma}^p$:

$$\Delta\sigma^p = \frac{4e^2\hbar^2}{\Delta m^2 c^2}\langle 1/r^3\rangle_0$$
$$\cdot \{[|S^{\pi\pi}_{10}|^2 + |S^{\sigma\sigma}_{10}|^2 - 2\sqrt{3}\,S^{\pi\pi}_{10}S^{\sigma\sigma}_{10} + \tfrac{1}{6}b^2]_{2\times Zn^{++}}$$
$$- [|S^{\delta\sigma}_{10}|^2 + (S^{\pi\pi}_{10} + S^{\sigma\sigma}_{10})^2]_{4\times K^+}$$
$$+ [|S^{\delta\sigma}_{10}|^2 + (S^{\sigma\sigma}_{10} - S^{\pi\pi}_{10})^2]_{2\times F^-}$$
$$+ [|S^{\delta\sigma}_{10}|^2 + (S^{\pi\pi}_{10} + S^{\sigma\sigma}_{10})^2]_{8\times F^-}\}\,, \quad (32)$$

$$\bar{\sigma}^p = -\frac{8}{3}\frac{e^2\hbar^2}{\Delta m^2 c^2}\langle 1/r^3\rangle_0$$
$$\cdot \{[|S^{\pi\pi}_{10}|^2 + |S^{\sigma\sigma}_{10}|^2 - 2\sqrt{3}\,S^{\pi\pi}_{10}S^{\sigma\sigma}_{10} + \tfrac{1}{6}b^2]_{2\times Zn^{++}}$$
$$+ 2[|S^{\delta\sigma}_{10}|^2 + (S^{\pi\pi}_{10} + S^{\sigma\sigma}_{10})^2]_{4\times K^+}$$
$$+ 2[|S^{\delta\sigma}_{10}|^2 + (S^{\sigma\sigma}_{10} - S^{\pi\pi}_{10})^2]_{2\times F^-}$$
$$+ 4[|S^{\delta\sigma}_{10}|^2 + (S^{\pi\pi}_{10} + S^{\sigma\sigma}_{10})^2]_{8\times F^-}\} \quad (33)$$

Several qualitative conclusions can be inferred from (32) and (33):

- The overlap contribution to $\Delta\sigma^p$ may be small due to cancellation between different contributions. The stronger is the cancellation, the more important is the covalent contribution to $\Delta\sigma^p$.

- For strong cancellation of overlap and weak covalency contributions, the calculated value of $\Delta\sigma^p$ is strongly dependent on the accuracy of the overlap integrals (see further below).
- The ratio $\Delta\sigma^p/\bar{\sigma}^p$ depends on neither Δ nor $\langle 1/r^3\rangle_0$. It is therefore well suited for comparison with the "semi-experimental" value obtained from line 5 of Table 1.

The overlap contributions $\Delta\sigma^p(O)$ and $\bar{\sigma}^p(O)$ contained in (32) and (33) are obtained by setting $b = 0$.

In order to estimate their size we used the following sources of overlap integrals: $F^- - F^-$ and $F^- - K^+$ overlaps were taken from [18] using the interpolation method proposed there; the $F^- - Zn^{++}$ overlaps were assumed to be equal to those calculated for $F^- - Ni^{++}$ in $KNiF_3$ [17]. The distances between different nuclei in $KNiF_3$ and $KZnF_3$ are practically the same since the unit cell dimensions are $a = 4.014$ Å and $a = 4.055$, respectively. The following numbers were used: $S^{\pi\pi} = 3.77$, $S^{\sigma\sigma} = 6.39$ for $F^- - Zn^{++}$, $S^{\pi\pi} = 1.379$, $S^{\sigma\sigma} = 5.546$, $S^{\delta\sigma} = 4.354$ for $F^- - K^+$ and $S^{\pi\pi} = 2.153$, $S^{\sigma\sigma} = 6.674$, $S^{\delta\sigma} = 3.824$ for $F^- - F^-$. All these values should be multiplied by 10^{-2}.

Using $\langle 1/r^3\rangle_0 = 43.2 \times 10^{24}\,\mathrm{cm}^{-3}$ and $\langle 1/r\rangle_0 = 2.196 \times 10^8\,\mathrm{cm}^{-1}$ from [4] and inserting in (32) to (33) the appropriate values of the overlaps one obtains: $\Delta\sigma^p(O) = -1.6 \times 10^{-17}\, 1/\Delta$, $\bar{\sigma}^p(O) = -1.7 \times 10^{-15}\, 1/\Delta$. The overlap contributions due to the two F^- at $(0, 0, \pm 1)$ were entirely negligible. The expressions for the diamagnetic parts which correspond to (32) − (33) are not given here for space reasons. They give:

$$\Delta\sigma^d(O) = 0.5\ \mathrm{ppm}\,, \quad \bar{\sigma}^d = 1.6\ \mathrm{ppm}\,.$$

As long as one neglects the covalent contribution, the following situation emerges:

- the diamagnetic overlap contributions to $\Delta\sigma$ and $\bar{\sigma}$ can safely be neglected as expected [15, 16].
- the ratio $\Delta\sigma^p(O)/\bar{\sigma}^p(O)$ obtained with the above mentioned overlap values is at variance with regard to sign and magnitude with the semiexperimental value of Table 1 which is -7.3×10^{-2}.

Therefore it seems that the covalent contribution cannot be neglected. An evaluation of b can be done if the ratio $\Delta\sigma^p/\bar{\sigma}^p$ as given by (32) and (33) is set equal to the semiexperimental value (-7.3×10^{-2}). One obtains $b = 0.13$.

Such a value is not unreasonable since in the closely related compound $KNiF_3$, covalency factors b^π and b^σ of 0.175 and 0.285 were obtained (see [17]).

On the other hand, it should be noted that moderate changes of overlap values may significantly alter the result. As an example we consider the case where the F−F overlaps are uniformly *increased* by 15% and the F−Zn and F−K overlaps are *decreased* by 15%. In this case $\Delta\sigma^p(O)/\bar{\sigma}^p(O) \approx -0.1$ and therefore covalency no longer needs to be invoked to explain the "semiexperimental" result. Such uncertainties may easily arise in overlap calculations and therefore we face the fact that for weakly covalent compounds in which $\Delta\sigma^p$ is small it is difficult to estimate the covalency contribution *only* from chemical shift data. In the case of $KZnF_3$, however, there exist NQR data which strongly indicate that covalency plays an important role. By NQR measurements on the ^{20}F-nuclei in $KZnF_3$ [6] it was found that the EFG at the F-site is $V_{zz} = +(7.7 \pm 1.7)\, 10^{17}\,\mathrm{V\,cm}^{-2}$. We calculated V_{zz} (see Appendix) using the same procedure as for $\boldsymbol{\sigma}$ and obtained

$$V_{zz} = V_{zz}(O) + \tfrac{4}{5}\, e \langle 1/r^3\rangle_0 \cdot \tfrac{1}{3}\,[b^2 + 2\sqrt{6}\, S_{10}^{4s,z}\, b]\,, \tag{34}$$

where $V_{zz}(O)$ is given by (A 12).

Neglecting the covalent contribution ($b = 0$) and using the same values of overlaps as for $\boldsymbol{\sigma}$ one obtains the overlap contribution to V_{zz}: $V_{zz}(O) \approx -10^{17}\,\mathrm{V\,cm}^{-2}$. On altering the value of the overlaps in the same way as was done tentatively above, the value of V_{zz} becomes even smaller. Therefore we conclude that a covalent contribution is essential to explain the experimental value of the EFG. As can be seen from (34) the covalent contribution is increasing the value of V_{zz} as is required by the experimental result. Unfortunately we have no knowledge of the overlap integral (F−Zn) $S_{10}^{4s,z}$ in (34) and therefore we can not evaluate V_{zz} using b obtained from the chemical shift data.

Conclusions

The anisotropy $\Delta\sigma$ of the fluorine chemical shift in $KZnF_3$ is small compared to $\sigma_\parallel$ and $\sigma_\perp$ on the absolute scale. The main part (57%) of $\Delta\sigma$ stems from closed shell electrons of neighbour ions ("geo-

metrical contribution"). This contribution is particularly important for $KZnF_3$ because of the filled 3d shell of Zn^{++}. In other ionic fluorides which have no ions with filled d shells the "geometrical contribution" is much weaker, in MgF_2, e.g., it contributes only 15% to $\Delta\sigma$ [4].

The remaining part of $\Delta\sigma$ as well as of $\bar{\sigma}$ is mainly paramagnetic and reflects the departure of the wavefunctions from their purely ionic form, e.g., through covalent mixing of wavefunctions on neighbouring ions. As long as covalency is assumed to give rise to bonding and antibonding states which both are fully occupied the covalency factor does not appear explicitly in the formula for $\Delta\sigma^p$ and $\bar{\sigma}^p$. In such a case $\Delta\sigma^p$ and $\bar{\sigma}^p$ depend only on overlap integrals between wavefunctions on neighbouring ions ("overlap contribution"). The result is then essentially equivalent to that obtained by using orthogonalized *ionic* functions (Löwdin's method) and not invoking at all the idea of covalent mixing.

Only bonding states with empty or partially filled antibonding counterparts bring a contribution to $\Delta\sigma^p$ which contains explicitly the covalency strength. The influence of such states to $\bar{\sigma}^p$ is, in general, much weaker. This is probably the reason why in many treatments of averaged chemical shifts in ionic crystals Löwdin's method was considered to be adequate [4, 15, 16]. When applied to $KZnF_3$ Löwdin's method allows a reasonable qualitative explanation of the small value of $\Delta\sigma^p$: overlap contributions from different neighbour ions tend to cancel each other.

Our calculations indicate that Löwdin's method is not sufficient to explain the experimental values of $\Delta\sigma$ and $\bar{\sigma}$ in $KZnF_3$ and that a covalent contribution from a (partially) occupied bonding state which has an empty antibonding counterpart needs to be taken into account. An estimate based on the "semiempirical" value of $\Delta\sigma^p/\bar{\sigma}^p$ gives a value for the respective covalency factor of $b = 0.13$.

An independent confirmation of this conclusion comes from the EFG at the F^--site determined by ^{20}F NQR in $KZnF_3$[6]. Neither its sign nor its magnitude can be explained if only Löwdin's orthogonalized wavefunctions, or filled bonding and antibonding pairs of states are considered.

Acknowledgements

We are indebted to Prof. H. Ackermann for making available to us a large piece of a single crystal of $KZnF_3$ which was originally prepared by Prof. Leckebusch/Bonn for the NQR studies. R. G. gratefully acknowledges stipends from the Deutsche Kernforschungsgesellschaft in Karlsruhe and it is his pleasure to express his gratitude to Prof. K. H. Hausser and the Max-Planck-Society for hospitality.

Appendix

Here we shall outline the procedure used to calculate $\boldsymbol{\sigma}$ (F) in the ZnF_6 fragment. It is based on a set of F^--ligand wavefunctions used previously for estimating other physical properties in such a fragment [17, 19]. It allows an easy separation of the overlap- and covalent bonding contributions to $\Delta\sigma^p$ and $\bar{\sigma}^p$. The EFG at the F^--site is calculated as well, using the same set of wavefunctions and approximations. The fluorines in the fragment are labelled as in [17] and [19]: F_1, F_4 sit on the x-, F_2, F_5 on the y-, and F_3, F_6 on the z-axis. F_3 is taken as the fluorine of interest. Hence overlaps of the form $S_{l3}^{\alpha\beta}$ are the same as $S_{l0}^{\alpha\beta}$ in the text. The central ion (Zn^{++}) as well as the ligand ($6F^-$) wavefunctions which transform according to the irreducible representations of O_h are given in Tables 23–26 of [19]. The ligand wavefunction of type S_r ($S_r = xy$, xz, etc.) belonging to the r-representation can be written

$$\chi(S_r, r) = [N(r)]^{-1/2} \sum_{l\alpha} A_l^{\alpha}(S_r, r)\, \varphi_l^{\alpha},$$

where $\varphi_l^{\alpha} = p_x(l), p_y(l), p_z(l)$. The amplitudes A_l^{α} are directly taken from Table 26 of [19]. For example

$$\chi(xz, t_{2g}^{\pi}) = [N(t_{2g}^{\pi})]^{-1/2} \cdot [p_x(3) - p_x(6) + p_z(1) - p_z(4)]$$

with

$$N(t_{2g}^{\pi}) = \tfrac{1}{4}[1 - S_{36}^{xx} + 2S_{31}^{xz}]^{-1} = \tfrac{1}{4}[1 + (S_{36}^{xx} - 2S_{31}^{xz}) + (S_{36}^{xx} - 2S_{31}^{xz})^2 + \ldots].$$

All overlap integrals appearing here are easily reduced to the usual overlaps $S^{\pi\pi}$, $S^{\sigma\sigma}$, $S^{\delta\sigma}$; e.g., $S_{3,6}^{xx} = S^{\pi\pi}$ for $F_3^- - F_6^-$. In the case of Zn^{++} we assume that only 3d electrons participate in forming bonding-antibonding pairs. Therefore only e_g and t_{2g} ligand and central ion wavefunctions couple (see Table 24 of [19]).

$$\psi^b(S_r, r) = [N^b(r)]^{-1/2}[\chi(S_r, r) + b(r)\, d(S_r, r)],$$
$$\psi^a(S_r, r) = [N^a(r)]^{-1/2}[d(S_r, r) - a(r)\, \chi(S_r, r)] \quad (A1)$$

with $r = e_g$; t_{2g} and $S_r = (d_{z^2}, d_{x^2-y^2})$; (d_{xz}, d_{yz}, d_{xy}). Orthonormality of ψ^b and ψ^a requires

$$N^b(r) = 1 + b^2(r) + 2b(r)\,S(r)\,,$$
$$N^a(r) = 1 + a^2(r) - 2a(r)\,S(r)$$

with

$$a(r) = [b(r) + S(r)]/[1 + b(r)\,S(r)]\,.$$

$S(r) = \langle \chi(r) \mid d(r) \rangle$ is easily expressed by the $S_{lc}^{\alpha\beta}$ between individual F^- and the central (c) Zn^{++}. Ligand orbitals not included in (A1) are unchanged.

As long as the bonding and antibonding as well as "free" ligand states are fully occupied the matrix elements of **P** corresponding to (A1) are

$$P_{lk}^{\alpha\beta} = \sum_{r,S_r} 1/N(r)\,[1/N^b(r) + a^2(r)/N^a(r)] \cdot A_l^\alpha(r,S_r)\,A_k^\beta(r,S_r)\,,\quad (l \neq c,\ k \neq c) \tag{A2}$$

$$P_{lc}^{\alpha\beta} = \sum_{r,S_r} 1/N(r)\,[b(r)/\sqrt{N^b(r)} - a(r)/\sqrt{N^a(r)}\,] \cdot A_l^\alpha(r,S_r)\,B_c^\beta(r,S_r)\,. \tag{A3}$$

B_c^β is defined as is A_l^β but refers to the central ion (c). In the weak covalency approximation a, b and S are assumed to be small and (A2) and (A3) reduce to

$$P_{lk}^{\alpha\beta}\ (l \neq c,\ k \neq c) = \sum_{r,S_r} 1/N(r)\,A_l^\alpha(r,S_r)\,A_k^\beta(r,S_r)\,[1 + S^2(r)]\,, \tag{A4}$$

$$P_{lc}^{\alpha\beta} = -\sum_{r,S_r} S(r)/\sqrt{N(r)}\ A_l^\alpha(r,S_r)\,B_c^\beta(r,S_r)\,. \tag{A5}$$

The first term in (A4) is due entirely to ligand states. Inserting (A4) and (A5) into (12)–(13) allows to separate the F^--ligand and the central ion contributions to $\boldsymbol{\sigma}^p$: $\boldsymbol{\sigma}^p = \boldsymbol{\sigma}^p(l) + \boldsymbol{\sigma}^p(c)$.

Using the values of the $A_l^\alpha(r,S_r)$ and $B_c^\beta(r,S_r)$ from Table (23–26) of [19] one obtains

$$\sigma_{xx}^p(c) = -\frac{2e^2\hbar^2}{\Delta m^2 c^2}\langle 1/r^3\rangle_0 \cdot [\,|S_{3c}^{z,z^2}|^2 + |S_{3c}^{z,yz}|^2 - 2\sqrt{3}\,S_{3c}^{z,z^2}\,S_{3c}^{z,yz}]\,,$$

$$\sigma_{zz}^p(c) = -\frac{2e^2\hbar^2}{\Delta m^2 c^2}\langle 1/r^3\rangle_0 \cdot [\,|S_{3c}^{x,xz}|^2 + |S_{3c}^{y,yz}|^2 - 2\,S_{3c}^{x,xz}\,S_{3c}^{y,yz}]\,.$$

Up to a factor of two this result is equivalent to (27). The factor of two originates in the different models used here and in the main text: In the ZnF_6 fragment considered here, the F^--ion of interest interacts with one Zn^{++} ion, whereas in the Zn^{++}–F^-–Zn^{++} subunit underlying (27) the F^--ion interacts with two Zn^{++} ions. The equivalence holds also for $\boldsymbol{\sigma}^p(l)$.

The fact that the final result is essentially equivalent to Löwdin's method is a consequence of (A3) which in the weak covalency approximation does not contain explicitly the covalency strength as long as bonding and antibonding states are fully occupied.

It does not hold if an antibonding state is, say, less occupied than its bonding counterpart. Such a case may arise if one considers the 4s excited state of Zn^{++}. It transforms according to A_{1g} of O_h and may form a bonding-antibonding pair of states when coupled to the "free ligand" $\chi(A_{1g})$ state. The population matrix elements become

$$P_{lk}^{\alpha\beta} = P_{lk}^{\alpha\beta}(O) + 2/[N(a_{1g})\sqrt{N^b(a_{1g})}] \cdot A_l^\alpha(a_{1g})\,A_k^\beta(a_{1g})\,,\quad (\text{for } l \neq c,\ k \neq c)\,,$$
$$P_{lc}^{\alpha\beta} = P_{lc}^{\alpha\beta}(O) + 2b/[N(a_{1g})\sqrt{N^b(a_{1g})}] \cdot A_l^\alpha(a_{1g})\,B_c^\beta(a_{1g})\,, \tag{A6}$$

where $P_{lk}^{\alpha\beta}(O)$ and $P_{lc}^{\alpha\beta}(O)$ are given by (A4) and (A5). Inserting (A6) into (12) and (13) gives

$$\sigma_{xx}^p = \sigma_{xx}^p(O) - \frac{4e^2\hbar^2}{\Delta m^2 c^2}\,\frac{1}{6}\,b^2(a_{1g})\,, \tag{A7}$$

$$\sigma_{zz}^p = \sigma_{zz}^p(O)\,. \tag{A8}$$

$\sigma_{xx}^p(O)$ and $\sigma_{zz}^p(O)$ are the contributions of the filled bonding/antibonding states as well as of states on the neighbouring ions which do not take part in the covalent bonding. These contributions are well described by (21). The second term of (A7) is due to the unfilled antibonding state A_{1g} arising from the 4s excited state of Zn^{++}.

According to the formalism used in this paper the EFG V_{zz} is given by

$$V_{zz} = -e\sum P_{lk}^{\alpha\beta}\,\langle \varphi_k^\beta \mid \frac{3z^2 - r^2}{r^5} \mid \varphi_l^\alpha \rangle\,. \tag{A9}$$

Neglecting small contributions from terms containing two center integrals (A9) reduces to

$$V_{zz} = -e\sum_{\alpha=x,y,z} P_{00}^{\alpha\alpha}\,\langle \varphi_0^\alpha \mid \frac{3z^2 - r^2}{r^5} \mid \varphi_0^\alpha \rangle \tag{A10}$$
$$= \tfrac{2}{5}\,e\,\langle 1/r^3\rangle_{F_{2p}}\,[P_{00}^{xx} + P_{00}^{yy} - 2P_{00}^{zz}]\,.$$

Using (A6) for the diagonal populations P_{00}^{zz}, (A10) can be brought to the form

$$V_{zz} = V_{zz}(\mathrm{O}) + \tfrac{4}{5}\, e \left\langle 1/r^3 \right\rangle_{\mathrm{F}_{2p}} \cdot \tfrac{1}{3}\left[b^2(\mathrm{a}_{1g}) + 2\sqrt{6}\, S_{10}^{4s,z}\, b(\mathrm{a}_{1g})\right], \qquad \text{(A11)}$$

where

$$V_{zz}(\mathrm{O}) = \tfrac{8}{5}\, e \left\langle 1/r^3 \right\rangle_{\mathrm{F}_{2p}} \cdot \{[(S_{10}^{\pi\pi})^2 - (S_{10}^{\sigma\sigma})^2]_{2\mathrm{Zn}^{++}} + [(S_{10}^{\sigma\sigma})^2 - (S_{10}^{\pi\pi})^2 + (S_{10}^{\delta\sigma})^2]_{4\mathrm{K}^{+}} - \tfrac{1}{2}[(S_{10}^{\pi\pi} + S_{10}^{\sigma\sigma})^2 + (S_{10}^{\delta\sigma})^2]_{8\mathrm{F}^{-}}\}. \qquad \text{(A12)}$$

$V_{zz}(\mathrm{O})$ has the same sources of contributions as $\sigma_{xx}^{p}(\mathrm{O})$. As can be seen from (A7) and (A11) the unfilled antibonding state A_{1g} makes a contribution which tends to *increase* both $\Delta\sigma^{p}$ and V_{zz}.

[1] M. Mehring, High Resolution NMR Spectroscopy in Solids, Springer-Verlag, Berlin 1976.
[2] U. Haeberlen, High Resolution NMR in Solids, Selective Averaging, Academic Press, New York 1976.
[3] Ref. [1], Table 5.4.
[4] R. W. Vaughan, D. D. Elleman, W.-K. Rhim, and L. M. Stacey, J. Chem. Phys. **57,** 5383 (1972).
[5] M. LeFloch-Durand, U. Haeberlen, and C. Müller, J. de Physique **43,** 107 (1982).
[6] H. Ackermann, D. Dubbers, M. Grupp, P. Heitjans, H. J. Stöckmann, K. P. Wanczek, K. Recker, and R. Leckebusch, Z. Naturforsch. **31a,** 1298 (1976).
[7] K. Knox, Acta Cryst. **14,** 583 (1961).
[8] D. K. Hindermann and C. D. Cornwell, J. Chem. Phys. **48,** 4148 (1968).
[9] N. F. Ramsey, Phys. Rev. **78,** 699 (1950).
[10] M. Karplus and T. P. Das, J. Chem. Phys. **34,** 1683 (1961).
[11] P.-Ö. Löwdin, Advan. Phys. **5,** 1 (1956).
[12] T. W. Sidwell and R. P. Hurst, J. Chem. Phys. **37,** 203 (1962).
[13] H. Post and U. Haeberlen, J. Magn. Reson. **40,** 17 (1980).
[14] Landolt-Börnstein, Numerical Data and Functional Relationships in Science and Technology, New Series, Vol. 8, p. 27ff., Springer-Verlag, Berlin 1976.
[15] D. Ikenberry and T. P. Das, J. Chem. Phys. **43,** 2199 (1965).
[16] V. M. Bouzmik and L. M. Avkhutsky, J. Mag. Reson. **5,** 63 (1971).
[17] R. G. Schulman and S. Sugano, Phys. Rev. **130,** 506 (1963); ibid. **130,** 517 (1963).
[18] D. W. Hafemeister and W. H. Flygare, J. Chem. Phys. **43,** 795 (1965).
[19] A. Abragam and B. Bleaney, Electron Paramagnetic Resonance of Transition Ions, Clarendon Press, Oxford 1970.